

## AN EXPERIMENTAL STUDY ON VISUAL COMFORT OF TUNNEL PORTALS IN VIRTUAL REALITY ENVIRONMENTS

ZHAO Weihao<sup>1</sup>, LIU Fang<sup>2</sup>, KONG Weijun<sup>3</sup>

**Abstract:** An appropriately-designed tunnel portal can provide drivers with a smooth visual transition and enhance driving comfort. However, with the increasing complexity of landscape elements, overly refined designs may distract drivers, potentially compromising driving safety. Despite this concern, research on the impact of different types of tunnel portal landscapes on drivers' visual comfort remains inadequate. It is worth exploring for identifying tunnel portal landscapes which distract drivers' attention and increase accident risk. A virtual experimental system based on VR (Virtual Reality) was configured to examine landscaping portals characterized by different styles. Electrodermal activity data, eye movement data, driving performance and subject data were collected for further analysis. The results showed that i) the distraction of landscaping portals to drivers varied under low and high-speed driving conditions, with distractions caused by refined type landscape being particularly noticeable, and drivers tend to more concentrate on driving with the increase of speed; ii) landscaping the portals will improve driving comfort, but the improving effect is less prominent in high-speed roads than low-speed roads; iii) driving safety and comfort decreased with the increase of speed under all three styles of tunnel portals, landscape design for tunnel portals should adapt to the design speed. The results of this investigation provide new insights into measures for improving the visual comfort of road tunnel portals.

**Keywords:** tunnel portal landscape; virtual reality (VR); visual comfort; safety

### 1. INTRODUCTION

With increasing implementation of human-centered design in infrastructure, tunnel portal design has been expanded beyond conventional safety requirements (Canto-Perello and Curiel-Esparza, 2001). Under the prerequisite of ensuring essential protective functions, the impact of portal environments on drivers' visual perception and psychological experience is now prioritized as a critical design factor (China Journal of Highway and Transport Editorial Department, 2022).

Well-designed tunnel portal landscapes significantly enhance driving comfort, and thus some scholars advocate incorporating substantial artificial elements to create elaborate landscapes (Chen and Yang, 2019; Wen et al., 2024). However, visually-striking landscapes may distract drivers, potentially increasing safety risks (Yuan, 2014). This perspective favors landscape strategies prioritizing natural ecological restoration (Ye et al., 2022). To support decisions on appropriate designs in tunnel portal landscapes, it is vital to develop tools for quantifying drivers' perception in driving environments.

This study developed a VR-based driving platform to investigate drivers' perception on three representative designs of a tunnel portal. The integrated experimental framework synchronizes VR scenarios, high-fidelity driving simulators, and multimodal biosensing to record real-time oculomotor patterns, EDA (electrodermal activity), and operational behaviors. The purpose of this study is quantitatively capture drivers'

<sup>1</sup> Graduate student, ZHAO Weihao, State Key Laboratory of Disaster Reduction in Civil Engineering, Tongji University, Shanghai 200092, China, zhaoweihaol031@163.com

<sup>2</sup> Professor, LIU Fang, State Key Laboratory of Disaster Reduction in Civil Engineering, Tongji University, Shanghai 200092, China, liufang@tongji.edu.cn

<sup>3</sup> MSc, KONG Weijun, State Key Laboratory of Disaster Reduction in Civil Engineering, Tongji University, Shanghai 200092, China, 2132417@tongji.edu.cn

psychophysiological responses to different designs of tunnel portals under various driving speeds. Findings from this study could support the principle of speed-adaptive design in tunnel portals.

## 2. METHODOLOGY

### 2.1. Experimental Setup

The configuration of the experimental system is illustrated in Figure 1a. To capture drivers' eye movement data in both simulated and real-world driving scenarios, an aSee VR eye tracker was employed, as shown in Figure 1b. The system was integrated with an HTC VIVE PRO virtual reality headset (Figure 1c) to ensure compatibility with the eye-tracking device. A Logitech G923 TRUEFORCE steering wheel (Figure 1d) was utilized to mimic driving feedback within the virtual environment. EDA data was used for a quantitative indicator of emotional responses under varying experimental conditions, and was recorded using ShimmerCapture v0.6 (Figure 1e).

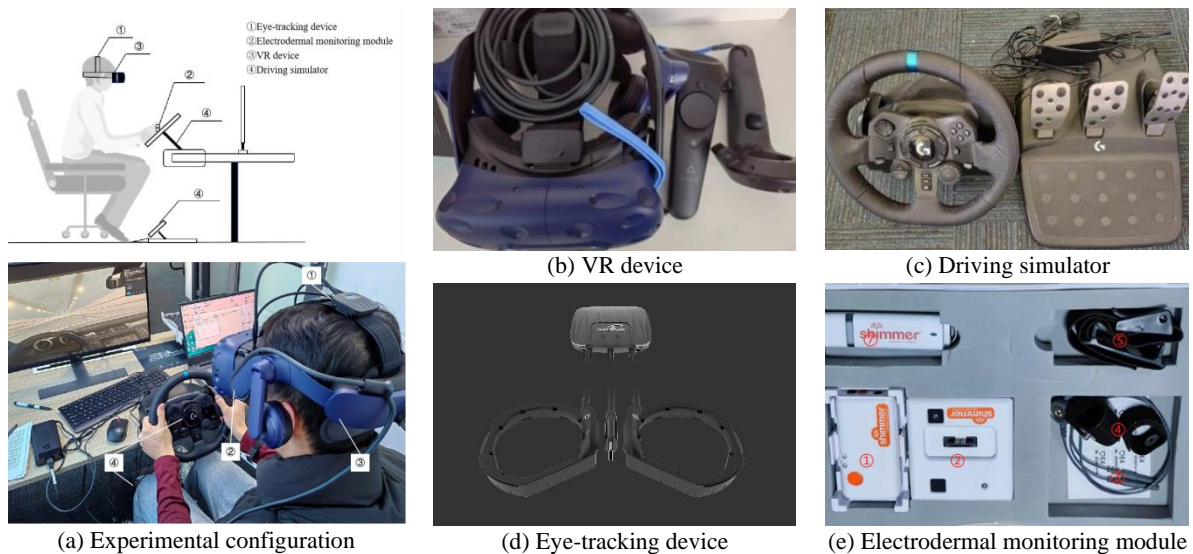


**Figure 1.** Experimental setup

### 2.2. Virtual displays

The virtual environment was constructed featuring a 35 m mountain elevation with 9.5 m high roadway slopes. The tunnel structure spans 600 m in length and 9.2 m in width with an external diameter of 12.7 m and internal diameter of 11.3 m, providing 7.5 m vertical clearance. The mountain massif and the tunnel were integrated into the Unity3D-based simulation platform.

Three tunnel portal landscape typologies (Figure 2) were engineered to assess driving safety-comfort relationships: Type I (Artificial Finishing Type), Type II (Natural Restoration Type), and Type III (Refined Landscape Type).

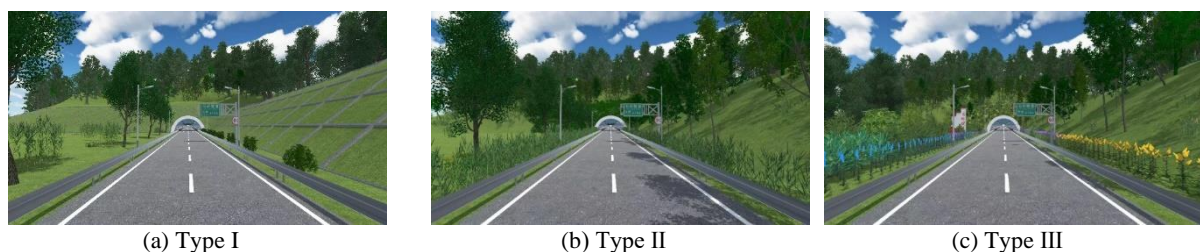


**Figure 2.** Three designs of the tunnel portal

As illustrated in Figure 3, the simulation environment is configured as a mountainous freeway section incorporating three 600-meter-long tunnels spaced at an interval of 1000 m. Each portal interface was programmed with modular switching capability among the three preset landscape typologies.

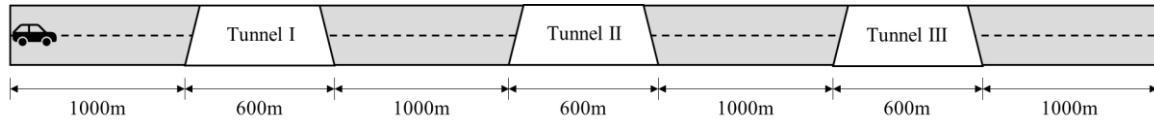


**Figure 3.** Basic scene

### 2.3. Testers

The experiment recruited 42 testers with driving experience. 男性23名，女性29名。To ensure the accuracy and reliability of the experimental data, testers were required to meet the following criteria: (1) a driving experience of at least one year, including experience driving through tunnel sections; (2) normal auditory, visual, and tactile perception abilities; (3) the capacity to clearly understand technical terms and verbally articulate their subjective experiences; and (4) adherence to a healthy and regular lifestyle for 24 hours prior to the formal trials to maintain physiological stability.

### 2.4. Experimental design

Prior to formal testing, testers completed operational training and signed informed consent forms alongside baseline demographic documentation. All collected information remained strictly confidential per consent agreements, accessible exclusively to research personnel. Then standardized training was administered covering experimental objectives, procedural workflows, VR equipment operation, and simulator controls to minimize cognitive biases. Pre-tests were conducted to enhance experimenters' operational proficiency, reduce procedure-related errors, and establish contingency protocols. The pre-test data were excluded from final analyses.

The formal experiment comprised three batches. Each participant completed four trial sequences as illustrated in Figure 4.

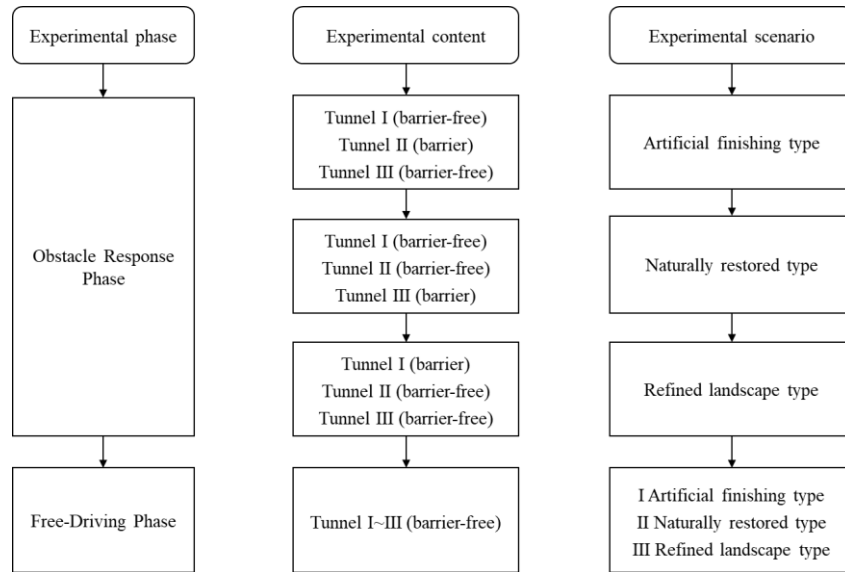


**Figure 4.** Flowchart of experimental design

### 2.5. Data collection

Data from 42 testers were collected across three modalities. Eye movement data were recorded using an eye tracker, extracting the number of fixation points during the 8-second period preceding each tunnel portal traversal. Driving behavior data were programmatically logged during both the obstacle-response and free-driving phases, yielding 6 trials per tester. Specifically, the obstacle-response phase dataset contained time stamps, speed, and positional parameters, while the free-driving phase recorded the average transit speed at portal traversals. EDA data were synchronously collected during the free-driving phase for each tunnel landscape type, with a per-recording acquisition duration of 8 seconds. Subjective data were collected using questionnaires administered immediately after participants completed a drive through each of the three tunnel types.

### 3. EVALUATION MODEL

#### 3.1. Delineating driving field of view

Based on cognitive psychology principles, the driving field of vision consists of a set of driver gaze points, with its distribution center defined as the gaze centroid (Lappi, 2016b; Lappi, 2022). As shown in Figure 5, the driving field of vision is characterized by the maximum horizontal gaze angle ( $\alpha'$ ) and maximum vertical gaze angle ( $\beta'$ ).

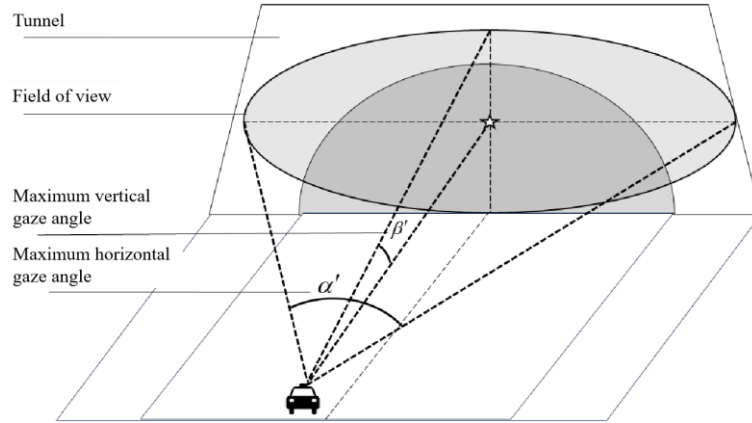


**Figure 5.** Schematic diagram of driving visual field

Figure 6 shows the driver's eye movement heatmap over a specific time period, where  $n$  and  $m$  represent the maximum horizontal and vertical distances of the gaze points from the screen center, respectively;  $\bar{n}$  and  $\bar{m}$  denote the horizontal and vertical distances of the gaze centroid from the screen center.

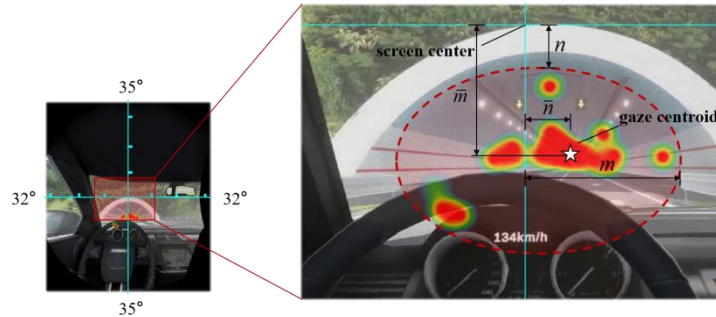


**Figure 6.** Calculation schematic of driving visual field range

The position coordinates of gaze points within the screen coordinate system are acquired using a VR eye tracker. Combined with the screen's field-of-view angles (32° horizontally per side, 35° vertically per side), viewing angle parameters relative to the screen center are calculated. To unify the reference to the gaze centroid, a viewing angle correction is applied via coordinate transformation.

The maximum Horizontal Gaze Angle Correction ( $\alpha'$ ) is computed as:

$$\alpha' = |\alpha - \bar{\alpha}| \times 2 \quad (1)$$

where  $\alpha$  is the maximum horizontal angle of gaze points relative to the screen center,  $\bar{\alpha}$  is the horizontal gaze angle of the gaze centroid relative to the screen center. They are computed as:

$$\alpha = \arctan\left(\frac{n \times \tan 32^\circ}{n_{\max}}\right) \quad (2)$$

$$\bar{\alpha} = \arctan\left(\frac{\bar{n} \times \tan 32^\circ}{n_{\max}}\right) \quad (3)$$

where  $n_{\max}$  is the horizontal distance from the screen center to the left/right edge (normalized to 0.5 for half-width).

Similarly, the maximum Vertical Gaze Angle Correction ( $\beta'$ ) is computed as:

$$\beta' = \beta - \bar{\beta} \quad (4)$$

where  $\beta$  is the maximum vertical angle of gaze points relative to the screen center,  $\bar{\beta}$  is the vertical gaze angle of the gaze centroid relative to the screen center.

$$\beta = \arctan\left(\frac{m \times \tan 35^\circ}{m_{\max}}\right) \quad (5)$$

$$\bar{\beta} = \arctan\left(\frac{\bar{m} \times \tan 35^\circ}{m_{\max}}\right) \quad (6)$$

where  $m_{\max}$  is the vertical distance from the screen center to the left/right edge.

### 3.2. Accessing driving safety

Driving safety is determined by the obstacle-response braking distance defined as the spatial interval between the braking initiation point and the obstacle. A scenario is classified as safe if the obstacle-response braking distance exceeds the safe stopping distance; otherwise, it is deemed hazardous. As illustrated in Figure 7, the obstacle-response braking distance and the driving speed are derived from testers' velocity-distance profiles during obstacle encounters. The inflection point on the curve indicates the braking initiation—corresponds to the obstacle-response speed (plotted on the x-axis) and braking distance (plotted on the y-axis).

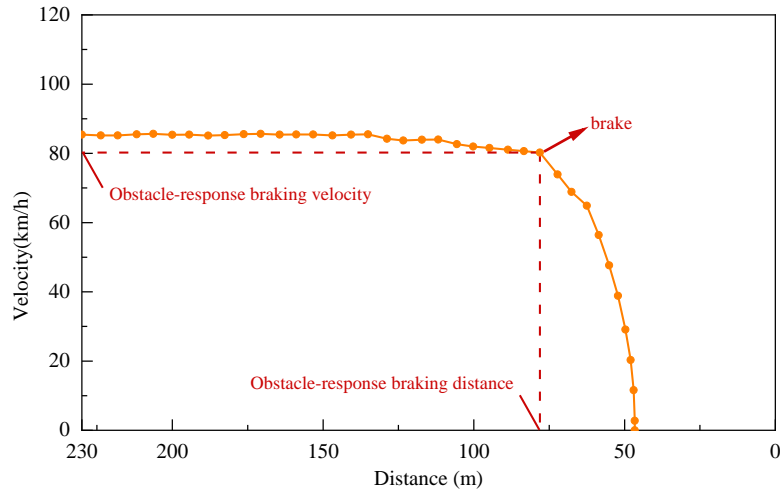


**Figure 7.** Calculation method of obstacle-response braking distance and speed

The safety stopping distance increases with the driving speed, and it can be calculated as follows :

$$S = v^2 / 2\mu g + S_0 \quad (7)$$

where  $v$  is the obstacle-response speed (m/s),  $\mu$  is the road friction coefficient (e.g., 0.8 for concrete surfaces),  $g$  is gravitational acceleration (9.8 m/s<sup>2</sup>), and  $S_0$  is the reserved safety distance (i.e., 20 m).

The obstacle-safety rate ( $\eta$ ) is defined as the ratio of safe trials to total trials:

$$\eta = \frac{p}{q} \quad (8)$$

where  $p$  is the number of safe scenarios, and  $q$  is the total number of trials.

The fixation frequency ( $k$ ) serves as another key metric for evaluating driving safety, demonstrating how information processing mechanisms affect safety performance. It can be computed as:

$$k = \frac{\sum_{i=1}^z P_i}{z \times t} \quad (9)$$

where  $P_i$  is the fixation count for the  $i^{\text{th}}$  tester,  $t$  is the eye-tracking data duration (i.e., 8 seconds in this study), and  $z$  is the total number of testers.

### 3.3. Assessing driving comfort

Driving comfort refers to the psychological state of relaxation and reduced tension experienced by drivers during vehicle operation, a subjective perception requiring integrated psychophysiological evaluation. This study adopts a combined approach of subjective questionnaires and EDA analysis.

Subjective questionnaires assess tunnel satisfaction and driving comfort based on the distribution and mean values of the five-point scale (2, 1, 0, -1, -2).

EDA-based comfort quantification relies on relative changes in skin potential difference. Figure 8 presents a typical EDA curve obtained from the experiment. Here we define a 100 m landscape section immediately before tunnel entry.

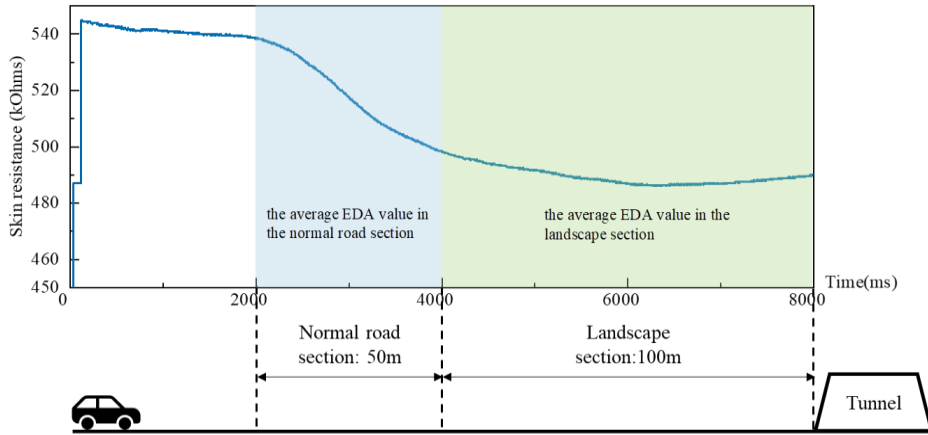


**Figure 8.** Schematic diagram of average electrodermal response calculation

The electrodermal response rate ( $\delta$ ) is calculated as:

$$\delta = (P' - P_0) / P_0 \quad (10)$$

where  $P'$  represents the average EDA value in the landscape section, and  $P_0$  denotes the baseline EDA value in the normal road section. Studies indicates (Posada-Quintero and Chon, 2020; Yan and Jia, 2022) that high electrodermal response rates correlate with heightened driver stress, inversely impacting comfort. Therefore, a positive  $\delta$  signifies tension, while a negative  $\delta$  indicates predominant comfort states.



## 4. RESULTS

### 4.1. Gaze Angle

Figure 9 illustrates the comparison of gaze angles as testers approached different tunnel portal types. For the Type III, mean maximum horizontal gaze angles were lower at close range and higher at greater distances. Under low-speed conditions, the Type I showed a significant increase in mean maximum horizontal gaze angles with increasing distance, consistent with the expansion of the visual field during near navigation. This increasing trend was even more pronounced under high-speed conditions.

For the Type III, a distinct inverse relationship between gaze angles and distance was observed during low-speed operation. This effect is attributed to the visual anchoring of composite landscape elements, which suppressed gaze dispersion. However, at high speeds, the stabilizing influence of the Type III was confined to the proximal segments near the portal. This targeted stabilization near the tunnel entrance effectively mitigates acute visual impacts for drivers during high-velocity approach.

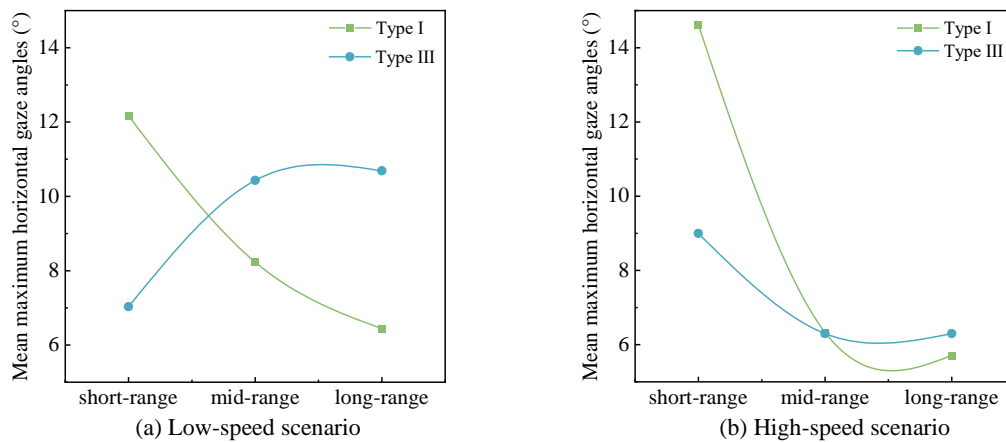


Figure 9. Average gaze angles of testers at different driving speeds

### 4.2. Fixation and Safety

Figure 10 reveals relationships between fixation frequencies and obstacle-safety rates across 3 tunnel portal types under low-speed and high-speed conditions. Under low-speed operations, Type I exhibited the highest obstacle-safety rate concurrently with the lowest fixation frequency; this combination indicates that its visually simplified design effectively reduces cognitive load, thereby enhancing safety margins. In contrast, both Type II and Type III showed progressively lower safety rates and higher fixation frequencies, confirming that increased landscape complexity under low speeds disperses driver attention, thus compromising safety performance. Conversely, under high-speed scenarios, Type II demonstrated optimal safety performance at moderately elevated fixation frequencies, suggesting its balanced visual complexity optimally directs attentional resources for proactive hazard detection. This analysis establishes that simplified landscapes (Type I) excel during low-speed approaches, whereas interfaces with moderated complexity (Type II) provide superior safety resilience in high-speed navigation.

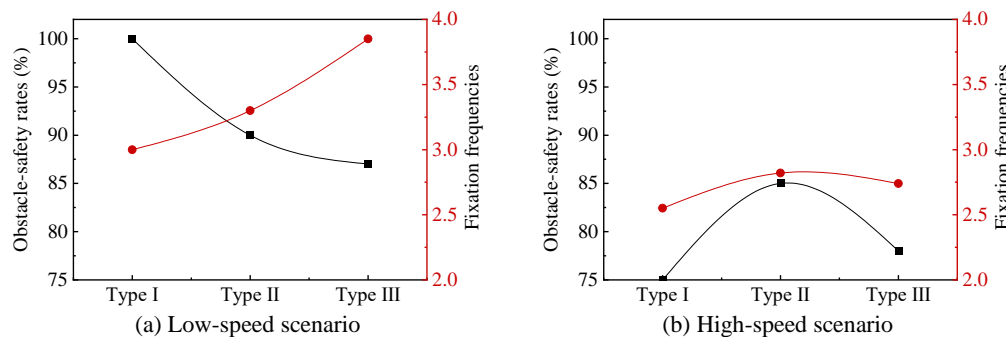
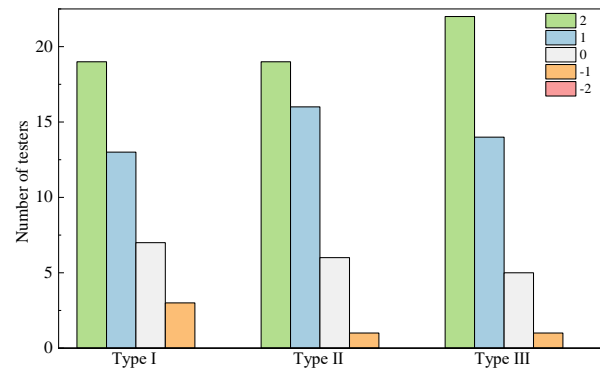


Figure 10. Average fixation frequencies and obstacle-safety rates of participants under different speed conditions

### 4.3. Speed Dependency and Driving comfort

Driving performance exhibited significant interactions between driving speed and portal landscape complexity, primarily affecting safety rates and driver comfort.

As illustrated in Figure 11, tunnels with refined landscape designs received significantly higher ratings in terms of driving comfort compared to those with artificial or natural restoration landscapes. These results suggest that visually enriched environments may have a more positive effect on drivers' perceptual comfort.



**Figure 11.** Subjective Ratings Distribution

As shown in Figures 12, under low-speed conditions, obstacle-safety rates decline progressively from Type I to Type III, while electrodermal responses concurrently rise, revealing a fundamental safety-comfort trade-off. Specifically, Type III maximizes driver comfort through optimized visual richness, yet this induces excessive cognitive engagement with environmental details, directly impairing hazard identification capacity and resulting in its lowest safety performance. Conversely, under high-speed operations, both metrics exhibit an inverted U-curve relationship with landscape complexity: Type II peaks at the curve apex with harmonized high safety and comfort, whereas Type I and Type III underperform at the curve troughs. This demonstrates that Type II's moderated visual complexity optimally balances cognitive load, avoiding attentional underload from sparse stimuli (Type I) while preventing overload from hypercomplexity (Type III).

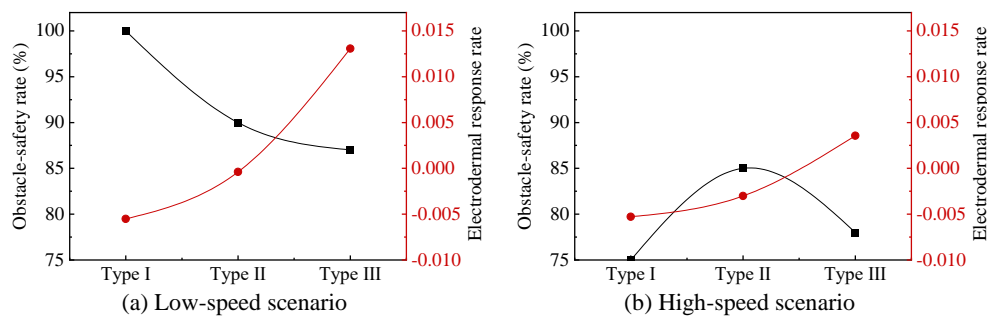


**Figure 12.** Obstacle-safety rates and electrodermal response rates of participants under different speed conditions

## 5. CONCLUSIONS

This study quantitatively investigated the impact of tunnel portal landscape design on drivers' visual comfort and safety across varying driving speeds using a comprehensive VR-based experimental approach. Through synchronized collection and analysis of eye movement data, EDA, and driving performance metrics from 42 participants navigating three distinct portal landscape typologies under controlled low- and high-speed conditions, we aimed to provide empirical evidence for speed-adaptive design strategies. This study reaches the following conclusions:

(1) The distraction caused by tunnel portal landscapes varies significantly with driving speed. Type III designs, while aesthetically engaging, led to noticeable visual distractions under low-speed conditions. However, drivers exhibited increased concentration at higher speeds, mitigating the adverse effects of complex visual stimuli.

(2) Landscaping tunnel portals generally enhanced driving comfort, particularly in low-speed scenarios. However, this improvement diminished on high-speed roads. Conversely, safety performance deteriorated with increasing speed across all landscape types, emphasizing the need for speed-adaptive design strategies.



(3) Landscape selection for tunnel portals is critically influenced by design speed. Under low-speed conditions, Type III designs significantly enhance driving comfort while preserving safety, as their moderate visual complexity prevents cognitive overload. In contrast, high-speed environments limit the comfort benefits of landscape interventions; here, Type II configurations achieve optimal safety-compatibility through ecological integration, balancing hazard anticipation with fatigue reduction.

## 6. BIBLIOGRAPHY

- [1] Canto-Perello, J., & Curiel-Esparza, J. (2001). Human factors engineering in utility tunnel design. *Tunnelling and Underground Space Technology*, 16(3), 211–215. [https://doi.org/10.1016/s0886-7798\(01\)00041-4](https://doi.org/10.1016/s0886-7798(01)00041-4)
- [2] China Journal of Highway and Transport Editorial Department. (2022). Review on China's traffic tunnel engineering research: 2022. *China Journal of Highway and Transport*, 35(4), 1-40. <https://doi.org/10.19721/j.cnki.1001-7372.2022.04.001>
- [3] Chen, F., & Yang, Y. (2019). Influence of tunnel entrance environment on driver's vision and physiology in mountainous expressway. *IOP Conference Series Earth and Environmental Science*, 295(4), 042138. <https://doi.org/10.1088/1755-1315/295/4/042138>
- [4] Wen, X., Ye, F., Su, E., Zhang, X., Han, X., Liu, J., & Zhu, W. (2024). Color design method for tunnel wall-type portals considering harmonization with time-varying environments: A study of driving simulation. *Tunnelling and Underground Space Technology*, 147, 105671. <https://doi.org/10.1016/j.tust.2024.105671>
- [5] Yuan Y. (2014). On the landscape design of mountain highway tunnel portals considering the psychological and physiological behaviors of a driver. *Modern Tunnelling Technology*, 51(3), 30-34. <https://doi.org/10.13807/j.cnki.mtt.2014.03.005>
- [6] Ye, F., Su, E. J., Liang, X. M., Zhang, X. B., Xia, T. H., & Wei, Y. C. (2022). Review and thinking on landscape design of highway tunnel. *China Journal of Highway and Transport*, 35(1), 23-37. <https://doi.org/10.19721/j.cnki.1001-7372.2022.01.003>
- [7] Lappi, O. (2022). Gaze Strategies in Driving - An Ecological Approach. *Frontiers in Psychology*, 13. <https://doi.org/10.3389/fpsyg.2022.821440>
- [8] Lappi, O. (2016b). Eye movements in the wild: Oculomotor control, gaze behavior & frames of reference. *Neuroscience & Biobehavioral Reviews*, 69, 49–68. <https://doi.org/10.1016/j.neubiorev.2016.06.006>
- [9] Yan, Y., & Jia, Y. (2022). A review on human comfort factors, measurements, and improvements in Human-Robot collaboration. *Sensors*, 22(19), 7431. <https://doi.org/10.3390/s22197431>
- [10] Posada-Quintero, H. F., & Chon, K. H. (2020). Innovations in Electrodermal Activity Data Collection and Signal Processing: A Systematic review. *Sensors*, 20(2), 479. <https://doi.org/10.3390/s20020479>